Sucrose acetate isobutyrate-based nanogels as liquid fiducial tissue markers with potential use in image guided radiotherapy

Bruun, Linda Maria; Schaarup-Jensen, Henrik; Jølck, Rasmus Irming; Hansen, Anders Elias; Christiansen, Anders N.; Scherman, Per Jonas Bengtsson; Clausen, Mads Hartvig; Kjær, Andreas; Andresen, Thomas Lars

Publication date:
2014

SUCROSE ACETATE ISOBUTYRATE-BASED NANOGELS AS LIQUID FIDUCIAL TISSUE MARKERS WITH POTENTIAL USE IN IMAGE GUIDED RADIOTHERAPY

Linda M. Bruun[1,2], Henrik Schaarup-Jensen[1,3], Rasmus I. Jølck[1,2], Anders E. Hansen[1,2], Anders N. Christiansen[4], Per Jonas Bengtsson Scherman[6], Mads H. Clausen[1,3], Andreas Kjær[5] and Thomas L. Andresen[1,2]

[1]Technical University of Denmark, Center for Nanomedicine and Theranostics, 2800 Kgs. Lyngby, Denmark
[2]Technical University of Denmark, Department of Micro-and Nanotechnology, 2800 Kgs. Lyngby, Denmark
[3]Technical University of Denmark, Department of Chemistry, 2800 Kgs. Lyngby, Denmark
[4]Technical University of Denmark, DTU Compute, Department of Applied Mathematics and Computer Science, 2800 Kgs. Lyngby, Denmark
[5]Rigshospitalet and University of Copenhagen, Department of Clinical Physiology, Nuclear Medicine & PET and Cluster for Molecular Imaging, 2100 Copenhagen, Denmark.
[6]Department of Oncology, Section of Radiotherapy, Rigshospitalet, 2100 Copenhagen, Denmark

The poster presents the development of a liquid fiducial tissue marker based on sucrose acetate isobutyrate (SAIB) and uniform, coated gold nanoparticles (AuNPs). The PNIPAM-coated AuNP-SAIB gel provided high CT contrast and high *in vivo* stability and was assessed to be a suitable tissue marker for image guided radiotherapy (IGRT).

Background

Within the field of radiotherapy, modern radiation oncology relies on high precision imaging techniques like Computed Tomography (CT), Positron Emitting Tomography (PET) and Magnetic Resonance Imaging (MRI) in order to deliver high radiation doses to precisely defined targets [1-3]. Tumors undergoing fractionated radiation therapy rarely display a fixed position during irradiation or within treatment, due to changes in organ filling, breathing motion and tumor size. This usually entails that the planning target volume has to be increased to ensure radiation dose coverage during treatment [4].

Image-guided Radiotherapy (IGRT) is a recently developed technique that has contributed to decrease in planning target volume, as 2D - and 3D images are frequently recorded before and during treatment [1,5]. This protocol has reduced treatment toxicity and improved relapse-free survival [6]. However, a remaining challenge within IGRT is fixation and correlation of the anatomical positions of several tumors to internal fixation points such as the skeleton. Radiopaque fiducial tissue markers (contrast agents) are therefore implanted near or inside the tumor to facilitate precise localization of tumors during therapy and thereby increase radiation accuracy. Solid markers like gold seeds are used routinely as radiopaque markers due to their excellent radiographic contrast, but the implantation procedure may cause severe complications [7]. Migration of seeds is likewise an issue. As an alternative, liquid fiducial markers are therefore of high interest.

Based on our previous work [8] - the work presented in this poster deals with development of biocompatible liquid fiducial injectable markers based upon well-defined coated gold nanoparticles (AuNPs) encapsulated within a secondary medium of sucrose acetate isobutyrate (SAIB), PLA (poly-lactic acid) and EtOH **(Figure 1)**. The mixture of PLA, EtOH, SAIB and coated AuNPs forms a Newtonian liquid (50-200 mPa·s) that is injectable through thin, hypodermic needles (25 G). Upon injection, efflux of EtOH via non-solvent induced phase separation (NIPS) occurs, leading to the formation of a highly viscous, hydrophobic fiducial radiopaque implant.

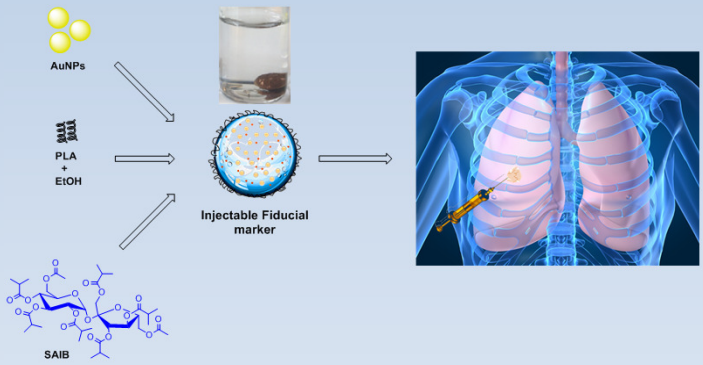

Figure 1. Principle of the developed liquid fiducial marker.

Experimental methods

The AuNPs were synthesized by a three step seeding protocol using chloroauric acid and trisodium citrate **(Scheme 1)**. Three different coating options were tested: 1) Thiol-terminated PEG_{5000} polymers, 2) thiol-terminated $PNIPAM_{3500}$ polymers and 3) a dithiolane functionalized SAIB derivative that was synthesized in 4 steps from sucrose.

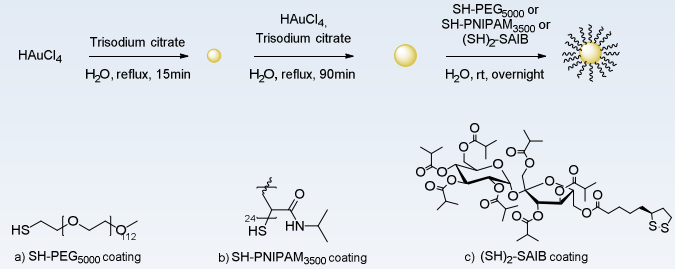

Scheme 1. Synthesis of PEG-, PNIPAM- and SAIB-coated AuNPs

The AuNP-SAIB gels were made by dispersing the coated AuNPs in EtOH follwed by mixing with SAIB and PLA. *In vitro* stability studies of AuNP-SAIB gels were conducted in PBS-buffer at 37°C. *In vivo* contrast and stability of the gels were monitored by micro-CT after injection of 200µL of SAIB/EtOH/PLA (75:20:5) + 30mg·mL^{-1} PNIPAM-AuNPs or 10mg·mL^{-1} PEG-AuNPs at the upper left flank of immunocompetent NMRI-mice. The X-ray contrast level, gel volume and gel homogeneity were evaluated over time by active contour model.

Results

Stable and uniform PEG - and PNIPAM-coated AuNPs were successfully synthesized, confer **Figure 2**. The dithiolane SAIB functionalized AuNPs were discarded due to observed aggregation of the nanoparticles. *In-vitro* stability test of the PEG-AuNP-SAIB gel (**Figure 3**) showed rapid burst release of PEGylated AuNPs. This burst release was completely avoided (<1%) with the PNIPAM-AuNP-SAIB gel, even with concentrations up to 100mg·mL^{-1}.

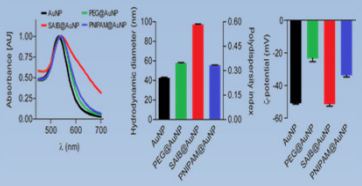

Figure 2. From left to right: UV-Vis -, DLS – and ζ-potential characterization of PEG-, PNIPAM- and dithiolane-SAIB coated AuNPs in aqueous solution

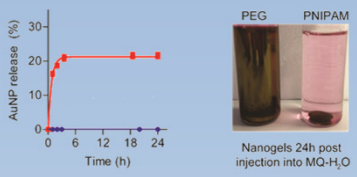

Figure 3. In vitro release in PBS-buffer at 37°C from SAIB/EtOH/PLA (75:20:5) containing either 30mg·mL^{-1} PNIPAM-AuNPs (blue) or 30mg·mL^{-1} PEGylated-AuNPs (red)

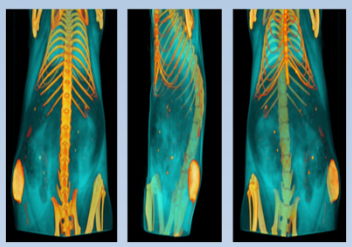

Figure 4. Maximum Intensity Projection of a PNIPAM-AuNP-SAIB gel–depot viewed from several angles

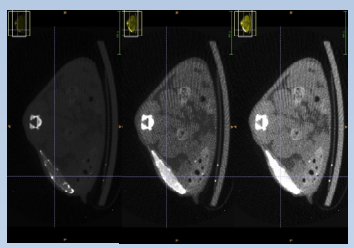

Figure 5. Micro-CT scanning slice of the PNIPAM-AuNP-SAIB gel in a mouse at three contrast levels. At high contrast level, slight inhomogeneity in the AuNP distribution is observed

In vivo contrast and stability of the PEG- and PNIPAM-AuNP-SAIB gels were likewise analyzed. The PEG-AuNP-SAIB gel suffered from PEG-AuNP migration towards the gel-boundaries over time [8]. **Figure 4** and **5** show micro-CT scans of mice after injection of the PNIPAM-AuNP-SAIB gel. The PNIPAM-AuNP-SAIB gel provided high stability *in vivo,* as well as a higher X-ray contrast level than the PEGylated AuNP-SAIB gel (as expected due to higher AuNP loading being possible with the PNIPAM coating).

The contrast level and homogeneity of the gels were analyzed manually in each CT scanning slice. First, a bounding box was drawn around each gel, and the gels were segmented by active contour model [9]. The median values of the two gel types were compared using a Wilcoxon rank-sum test [10]. The homogeneity of the gels was then analyzed by first applying a Box-Cox transformation [11] to the two datasets for variance stabilization, followed by a Wilcoxon rank sum test for comparison of variance.

The PNIPAM-AuNP-SAIB gel had a significantly higher median (P-value: 0.0006) as expected due to higher loading of AuNPs. Despite a much better contrast, surprisingly no significant difference was found in the variance of the gels (P-value: 0.0734), thereby indicating the same extent of inhomogeneity in the PNIPAM-AuNP-SAIB gel and the PEG-AuNP-SAIB gel. This is due to the inhomogeneity only being visible at higher intensity levels (**Figure 5**). Due to the much lesser resolution in clinical imaging systems, the slight inhomogeneity of the PNIPAM-AuNP-SAIB gel will not be visible and will therefore not be an issue in clinical applications.

Handling of PNIPAM-coated AuNPs was furthermore superior to the PEGylated AuNPs, as they can be lyophilized and stored as a stable powder, that is easily dispersible in EtOH. Based on the presented *in vitro* and *in vivo* results, the PNIPAM-AuNP-SAIB gel was evaluated to be suitable as tissue marker for IGRT.

References

[1]: L. A. Dawson, M. B. Sharpe, *Lancet Oncol*. **2006**, *7*, 848
[2]: J. Bussink, J. H. A. M. Kaanders, W. T. A. van der Graaf, W. J. G. Oyen, *Nat. Rev. Clin. Oncol*. **2011**, *8*, 233
[3]: D. Verellen, R.M. De, N. Linthout, K. Tournel, G. Soete, G. Storme, *Nat. Rev. Cancer*, **2007**, *7*, 949
[4]: K. M. Langen, D. T. Jones, *Int. J. Radiat. Oncol. Biol. Phys.* **2001**, *50*, 265
[5]: M. Falk, P. M. af Rosenschold, P. Keall, H. Cattell, B. C. Cho, P. Poulsen, S. Povzner, A. Sawant, J. Zimmerman, S. Korreman, *Radiother. Oncol*. **2010**, *94*, 218
[6]: M. J. Zelefsky, M. Kollmeier, B. Cox, A. Fidaleo, D. Sperling, X. Pei, B. Carver, J. Coleman, M. Iovelock, M. hunt, *Int. J. Radiat. Oncol. Biol. Phys*. **2012**, *84*, 125
[7]: N. Bhagat, N. Fidelman, J. C. Durack, J. Collins, R. L. Gordon, J. M. LaBerge, R. K. J. Kerlan, *Cardiovasc. Intervent. Radiol.* **2010**, *33*, 1186
[8]: R. I. Jølck, T. Binderup, A.E. Hansen, et al. *Adv. Healthcare Mater.* **2014,** 1
[9]: T. F. Chan, L. A. Vese, *Image Processing, IEEE Transactions on*, **2001**, *10 (2)*, 266
[10]: F. Wilcoxon, *Biometrics 1.6* **1945,** 80
[11]: G. E. P. Box , D. R. Cox, *J. R. Stat. Soc., Series B 26.2* , **1964,** 211.

Acknowledgements

The authors wish to thank the Nanoguide project and the Danish Council For Strategic Research for financing this project.